Available online at www.sciencedirect.com

ScienceDirect

Proceedings of the Combustion Institute 000 (2018) 1–9

Proceedings of the Combustion Institute

www.elsevier.com/locate/proci

A molecular dynamics study of fuel droplet evaporation in sub- and supercritical conditions

Guowei Xiao [a,b], Kai H. Luo [a,c,*], Xiao Ma [b], Shijin Shuai [b]

[a] *Center for Combustion Energy, Key Laboratory for Thermal Science and Power Engineering of Ministry of Education, Department of Energy and Power Engineering, Tsinghua University, Beijing 100084, China*
[b] *State Key Laboratory of Automotive Safety and Energy, Tsinghua University, Beijing 100084, China*
[c] *Department of Mechanical Engineering, University College London, Torrington Place, London WC1E 7JE, UK*

Received 30 November 2017; accepted 9 September 2018
Available online xxx

Abstract

Evaporation processes of a fuel droplet under sub- and supercritical ambient conditions have been studied using molecular dynamics (MD) simulations. Suspended n-dodecane droplets of various initial diameters evaporating into a nitrogen environment are considered. Both ambient pressure and temperature are varied from sub- to supercritical values, crossing the critical condition of the chosen fuel. Temporal variation in the droplet diameter is obtained and the droplet lifetime is recorded. The time at which supercritical transition happens is determined by calculating the temperature and concentration distributions of the system and comparing with the critical mixing point of the n-dodecane/nitrogen binary system. The dependence of evaporation characteristics on ambient conditions and droplet size is quantified. It is found that the droplet lifetime decreases with increasing ambient pressure and/or temperature. Supercritical transition time decreases with increasing ambient pressure and temperature as well. The droplet heat-up time as well as subcritical to supercritical transition time increases linearly with the initial droplet size d_0, while the droplet lifetime increases linearly with d_0^2. A regime diagram is obtained, which indicates the subcritical and supercritical regions as a function of ambient temperature and pressure as well as the initial droplet size.

Keywords: Droplet; Evaporation; Supercritical condition; Molecular dynamics simulations

1. Introduction

Droplet evaporation occurs in many liquid-fueled propulsion systems, such as diesel engines and liquid rocket engines, and has major influence on the mixture formation and the subsequent combustion process. Many of these combustion systems operate at chamber pressures that exceed the critical pressure of the injected fuel. As a result, the

* Corresponding author at: Department of Mechanical Engineering, University College London, Torrington Place, London, WC1E 7JE, UK.
E-mail address: k.luo@ucl.ac.uk (K.H. Luo).

https://doi.org/10.1016/j.proci.2018.09.020
1540-7489 © 2018 by The Combustion Institute. Published by Elsevier Inc.

fuel droplets may undergo a transcritical evaporation process, in which transition from liquid to supercritical phase happens at the droplet surface.

Drastic changes in fluid properties happen when its thermodynamic critical point is approached. For example, it is well known that surface tension and latent heat diminish, while constant-pressure specific heat becomes very large in the transcritical regime. As a result, fuel jets in supercritical environment exhibit characteristics of a turbulent gas jet, with disappeared liquid-gas interface and suppressed liquid atomization, as described by previous studies of Mayer et al. [1] and Chehroudi et al. [2]. Moreover, the conventional droplet evaporation theory [3], in which liquid and vapor phases are treated separately and the quasi-steady approximation of the vapor phase is applied, may not be valid under supercritical ambient conditions.

The attempt to study the evaporation of a fuel droplet in supercritical environment was perhaps initiated by Spalding [4]. In his work the droplet was treated as a point source of dense gas with constant physical properties. The same problem was re-examined by many researchers, with the thermodynamic and transport properties of the fluid carefully evaluated and other problems posed by high pressure accounted for. Most of them considered a single suspended drop composed of liquid oxygen [5–7] or hydrocarbon fuel [8–19]. Notably, the study of Rosner et al. [9] was perhaps the first to take into account the solution of ambient gas in liquid phase, and the first to discuss the conditions under which the droplet surface may be heated to the critical state. Yang et al. [5] proposed a unified thermophysical property evaluation scheme based on real-fluid equation of state and corresponding state theory. Harstad and Bellan et al. [7,17] incorporated Soret and Dufour effects and thermodynamic non-equilibrium in their model. The effects of gas-phase unsteadiness were addressed by Zhu [15] and Aggarwal [18]. Although these modeling works are sophisticated and help with understanding the evaporation phenomena under high pressure conditions, they need to invoke some limiting assumptions. Many simulations adopted truncated property evaluation schemes, or employed empirical correlations extrapolated from low-pressure conditions, thus introduced a number of uncertainties into the model.

Experimental measurements have also been carried out with the hope of obtaining useful data for estimation of droplet evaporation behavior and evaluation of numerical models. However, most of them employed suspended millimeter-size droplet [8,20,21], thus effects of natural convection cannot be ignored especially when the ambient pressure is high. On the contrary, droplets in sprays are so fine that influence of convection on droplet evaporation is negligible. Therefore, experiments in a microgravity conditions [22–26] are more suitable for validation of theoretical and numerical models. In a recently published paper of Nomura et al. [25], n-hexadecane droplet was employed and temporal variations in droplet diameter were successfully obtained for evaporations under supercritical conditions. Despite the fact that many useful data have been obtained, experimental studies are unable to measure many key parameters in an unsteady process of micro- and nano-droplets. As an example, temperature distribution of an evaporating droplet can hardly be measured. Therefore, the time when supercritical state is attained cannot be determined accurately.

To avoid the problems encountered by continuum-based simulations and experiments, discrete simulation techniques like molecular dynamics (MD) simulations were used to examine the evaporation behavior. Kaltz et al. [27] was perhaps the first to investigate the supercritical evaporation phenomenon using MD simulations. In their study, the evaporation of a liquid oxygen droplet into quiescent environments comprised of either hydrogen or helium was investigated. Consolini et al. [28] simulated the evaporation of submicron xenon droplets in nitrogen ambient under sub- and supercritical ambient conditions. In a recent study by Mo et al. [29] the evaporation of three normal alkanes (n-heptane, n-dodecane and n-hexadecane) under engine relevant conditions was investigated. However, an evaporating liquid film was used, rather than an evaporating droplet, which is of greater practical significance.

In the present study, the evaporation of a fuel droplet was investigated. Nitrogen was used as ambient gas and n-dodecane (critical temperature: 658 K; critical pressure: 1.82 MPa) was used as a surrogate fuel. The same system have been extensively investigated to understand its phase equilibria and interfacial properties by theoretical calculation [30], MD simulation [29,31], as well as experiments [32]. In the present study, emphasis was placed on the dependence of attainment of supercritical transition on ambient conditions (pressure and temperature), with the influence of the initial droplet size also taken into account. One important drawback of MD is the high computational cost. As a result, the spatial and temporal scales of the simulations are usually limited to a few hundred nanometers and nanoseconds, respectively. Therefore, it is necessary to explore the validity of extending those observed sub-micron phenomena to macro system by studying the behavior of various sized droplets.

The purpose of the present paper is to study the evaporation of a fuel droplet under supercritical conditions, and provide data for evaluation of numerical models of fuel droplet evaporation under modern diesel engine relevant conditions. The droplet lifetime and supercritical transition time are obtained from variations of droplet size and

Please cite this article as: G. Xiao, K.H. Luo and X. Ma et al., A molecular dynamics study of fuel droplet evaporation in sub- and supercritical conditions, Proceedings of the Combustion Institute, https://doi.org/10.1016/j.proci.2018.09.020

Table 1
Simulation details.

Droplet size, nm	21	30	43
Number of molecules in the drop	12,455	37,359	106,143
Simulation box size, nm^3	60^3	80^3	120^3
Reduced ambient pressure	2.22–9.28	0.57–9.10	2.34–9.26
Reduced ambient temperature	0.91–1.67		
Package	LAMMPS		

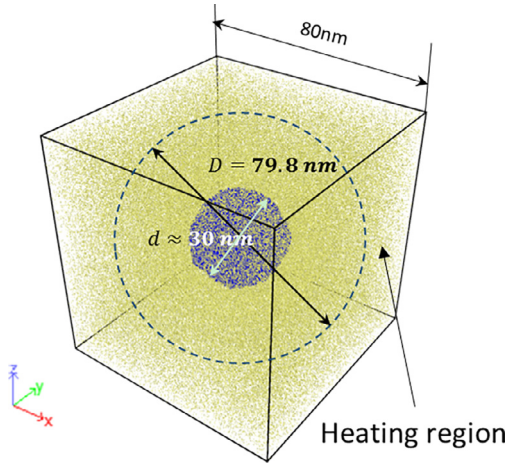

Fig. 1. Initial configuration of the simulation setup (Medium droplet).

temperature and concentration distributions. And their dependence on the ambient and droplet size is discussed.

2. Simulation method

2.1. Simulation details

In the present study, a single suspended n-dodecane droplet surrounded by a nitrogen ambient in a cubic simulation box was considered. The initial configuration of the system is illustrated in Fig. 1. The n-dodecane droplet and nitrogen ambient gas were first simulated separately until both reached the equilibrium states. Then the fuel droplet was placed in the center of the nitrogen ambient, with the nitrogen molecules in that region deleted to avoid molecule overlap. The initial temperature of the droplet is 363 K, which is close to the temperature of the injected fuel of real internal combustion engines. The initial temperature of the ambient gas is determined by the target ambient condition, and the pressure is controlled by the number of nitrogen molecules.

The simulations were performed using the micro-canonical ensemble (NVE). The periodic boundary condition was used in all three directions. To maintain a constant 'far-field' temperature, the outermost region of the simulation box was defined as the 'heating region', in which the velocity of the molecules was rescaled every timestep. In addition, those n-dodecane molecules which entered the heating region were deleted. By this means, the influence of vapor phase fuel molecules was removed, and the evaporation can be regarded as happening in an infinite space. It should be noted that, ambient pressure, as well as the gradients of temperature and species mole fractions, may decrease upon evaporation, due to the regression of the droplet surface. However, the droplet only accounts for less than 3% of the volume of the simulation box, thus those variations are negligible.

The target ambient conditions considered in this study ranged from subcritical to supercritical, as summarized in Table 1. Here the reduced pressure p_r and reduced temperature T_r were both calculated by dividing the values by the critical values of n-dodecane. Simulations were performed on a Cray XC30 supercomputer. Each case of the large, medium and small droplets was run using 10 nodes, 4 nodes, and 2 nodes, respectively, with one node having 24 cores and 64 GB memory. The wall time for one case is about 10 h.

The united atom model was used to describe n-dodecane molecules. This model is based on the observation that the C–H bond in hydrocarbon molecules is much shorter and stronger than the C–C bond, thus methyl (CH_3) or methylene (CH_2) groups are treated as separate atom-like structures. The interaction between un-bonded 'atoms' was described by the 12–6 Lennard–Jones potential:

$$U^{LJ}(r_{ij}) = 4\varepsilon_{ij}\left[\left(\frac{\sigma_{ij}}{r_{ij}}\right)^{12} - \left(\frac{\sigma_{ij}}{r_{ij}}\right)^{6}\right] \quad (1)$$

where the energy parameters $\varepsilon_{CH_3} = \varepsilon_{CH_2} =$ 468.6 J/mol, the size parameters $\sigma_{CH_3} = \sigma_{CH_2} =$ 0.401 nm, r_{ij} is the distance between atoms. Bond stretching is described by a harmonic potential:

$$U^{s}(r) = k_b(r - r_0)^2, \quad (2)$$

where the stretching coefficient $k_b = 1.464 \times 10^5$ kJ/(mol · nm^2), r is the distance between the two bonded atoms, $r_0 = 0.153\,nm$ is the equilibrium bond distance. Bond bending is also described by a

Please cite this article as: G. Xiao, K.H. Luo and X. Ma et al., A molecular dynamics study of fuel droplet evaporation in sub- and supercritical conditions, Proceedings of the Combustion Institute, https://doi.org/10.1016/j.proci.2018.09.020

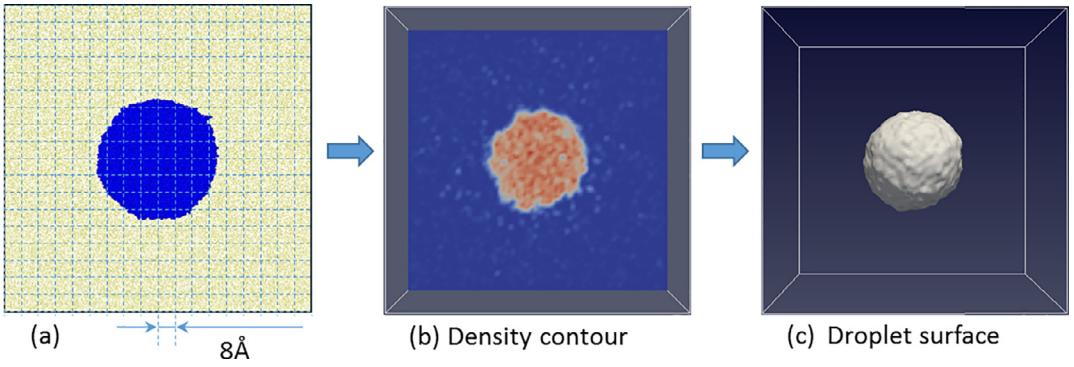

Fig. 2. Droplet diameter calculation.

harmonic potential:

$$U^b(\theta) = k_\theta(\theta - \theta_0)^2 \quad (3)$$

where the bending coefficient $k_\theta = 251$ kJ/(mol · rad^2), θ is the angle formed by three bonded atoms, and $\theta_0 = 109^\circ$ is the equilibrium angle. The OPLS torsional potential is used to describe the bond torsion interactions:

$$U^t(\emptyset) = 0.5k_1(1 + cos\emptyset) + 0.5k_2(1 - cos2\emptyset) + 0.5k_3(1 + cos3\emptyset) \quad (4)$$

where $k_1 = 5.904$ kJ/mol, $k_2 = -1.134$ kJ/mol, $k_3 = 13.159$ kJ/mol, $\emptyset$ is the dihedral formed by 4 bonded atoms.

Nitrogen molecules were regarded as two separate interaction sites connected by a fixed bond [33]. The non-boned interactions are again characterized by the 12–6 Lennard–Jones potential, with parameters $\varepsilon_N = 0.3026$ kJ/mol and $\sigma_N = 0.332$ nm. The distance between two bonded nitrogen atoms is constrained at 1.106 Å. The Lorentz–Berthelot mixing rule is used to obtain the interaction parameters between different atoms:

$$\varepsilon_{ij} = \sqrt{\varepsilon_i \cdot \varepsilon_j}, \quad \sigma_{ij} = (\sigma_i + \sigma_j)/2 \quad (5)$$

In an earlier publication of the authors [34], the present intermolecular potential model was validated by a liquid-vapor phase equilibrium calculation of the n-dodecane-nitrogen system. The results were shown to be in good agreement with experimental data by García-Cordova et al. [32].

2.2. Data processing

In the present study, the temporal variation in the droplet diameter is obtained by the following processes. As illustrated in Fig. 2a, the simulation box is divided into 8 Å × 8 Å × 8 Å grids, the density of fluid in each grid is calculated by counting the number of atoms in it, thus the density contour (Fig. 2b) of the system can be obtained. The droplet-ambient boundary is defined as the surface where the fluid density equals the mean value of the maximum and the minimum densities of the system (Fig. 2c). The droplet volume is then calculated, and the droplet diameter is defined as the diameter of a sphere of identical volume as the droplet.

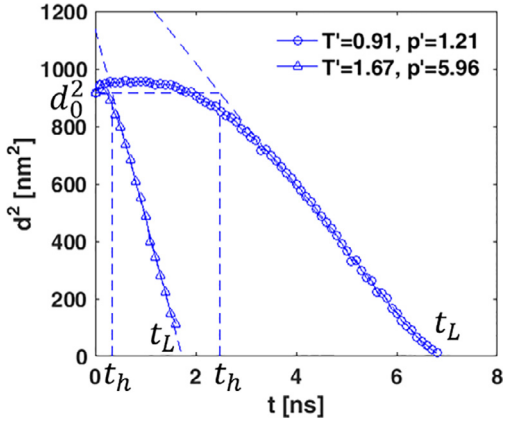

Fig. 3. Temporal variation of the square of droplet diameter.

Following the above procedures, the droplet diameter history was successfully obtained. The conventional droplet evaporation theory stated that the square of the droplet diameter (d^2) decreases linearly with time in the quasi-steady evaporation period. Therefore, d^2 was plotted as a function of time, as illustrated in Fig. 3. It is evident that d^2 indeed decreases linearly after the initial droplet heat-up period and before the end of evaporation, even though the ambient condition was well beyond the critical point of the fuel (e.g., $T' = 1.67$, $p' = 5.96$). Figure 3 also illustrates the definition of evaporation rate constant k, initial heat-up period t_h and droplet lifetime t_L. The method is similar to that used by Nomura et al. [25]. Linear least square fitting was performed in the range between 0.862 d^2

Please cite this article as: G. Xiao, K.H. Luo and X. Ma et al., A molecular dynamics study of fuel droplet evaporation in sub- and supercritical conditions, Proceedings of the Combustion Institute, https://doi.org/10.1016/j.proci.2018.09.020

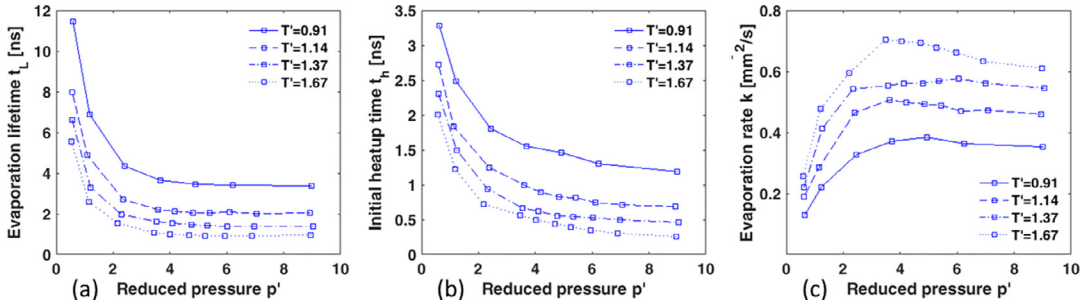

Fig. 4. (a) Droplet lifetime, (b) initial heat-up time and (c) evaporation rate constant as a function of reduced ambient pressure.

and 0.215 d^2 (that is, 80% and 5% of the initial droplet volume), and evaporation rate constant k was defined as the slope of the straight line. The initial heat-up time and evaporation lifetime were defined as the time of the intersection between the straight line and the line $(d/d_0)^2 = 1$ and $d^2 = 0$, respectively.

3. Results and discussion

3.1. Effects of ambient temperature and pressure

In the present study, simulations of the medium-size droplet were performed under the widest ambient condition range. Figure 4 shows the variation of the droplet lifetime t_L, initial heat-up time t_h and evaporation rate constant k as a function of reduced ambient pressure. It is not surprising that droplet lifetime decreases with increasing ambient temperature. When the ambient temperature is increased, both heat transfer from the gas phase to the liquid phase and mass diffusion are promoted. These observations are further confirmed by the decreased initial heat-up time (Fig. 4b) and increased evaporation rate constant (Fig. 4c).

Note that under all ambient temperatures investigated here, droplet lifetime decreases monotonically with increasing ambient pressure as shown in Fig. 4a. In some previous studies [14,21,22], it was observed that under low subcritical temperatures, droplet lifetime first increases and then decreases with increasing ambient pressure. They attributed this increase in droplet lifetime to the combined effects of decreasing mass diffusivity and increasing boiling point of the liquid with increasing ambient pressure. However, in the present study the investigated temperatures are relatively high ($T' \geq 0.91$), and the effect of decreasing latent heat of evaporation with ambient pressure overtakes other factors, leading to decreased lifetime with increasing ambient pressure. Another finding of the present study is that the evaporation rate constant first increases and then decreases with increasing ambient pressure (Fig. 4c). The increase in the evaporation rate constant at relatively lower pressures can be attributed to the increase in the thermal conductivity of the fuel/nitrogen mixture and the decrease in the latent heat of evaporation when the ambient pressure is increased. Increased heat conductivity also decreases the initial heat-up time, as shown in Fig. 4b. As a result of the combined effects of decreasing heat-up time and increasing evaporation rate, droplet lifetime decreases rapidly with increasing ambient pressure. However, when ambient pressure further increases, binary mass diffusion coefficient decreases and the equilibrium mole fraction of fuel at the droplet surface decreases, and consequently the evaporation rate constant k decreases with increasing pressure. The non-linear dependence of evaporation rate constant k on ambient pressure was also observed in the experiments of Sato et al. [22] and Nomura et al. [25]. The effects of decreased heat-up time and decreased evaporation rate cancel each other, and the evaporation lifetime becomes almost pressure-independent at high ambient pressures. Figure 4c shows that k of n-dodecane droplets at an ambient temperature of 750 K ($T' = 1.14$) and an ambient pressure of 1 MPa-4 MPa ($p' = 0.57$–2.2) falls in the range of 0.19 mm^2/s-0.46 mm^2/s, while the measured evaporation constants of n-heptane [22] and n-hexadecane [25] at 773 K and similar ambient pressures fall in the range of 1.6 mm^2/s-2.5 mm^2/s and 0.18 mm^2/s-0.29 mm^2/s, respectively. Considering the difference in volatility of n-dodecane with those fuels and slightly lower ambient temperature, the calculated results in the present study are fairly acceptable.

In order to estimate the time when supercritical transition happens, a method proposed by Mo et al. [29] is utilized. The droplet was assumed to be spherically symmetry during the evaporation process, thus the thermodynamic properties of the fluid at a given time were calculated as a function of the radial distance from the droplet center. As a result, the correlation between fluid temperature T and mole fraction of n-dodecane x_n

Please cite this article as: G. Xiao, K.H. Luo and X. Ma et al., A molecular dynamics study of fuel droplet evaporation in sub- and supercritical conditions, Proceedings of the Combustion Institute, https://doi.org/10.1016/j.proci.2018.09.020

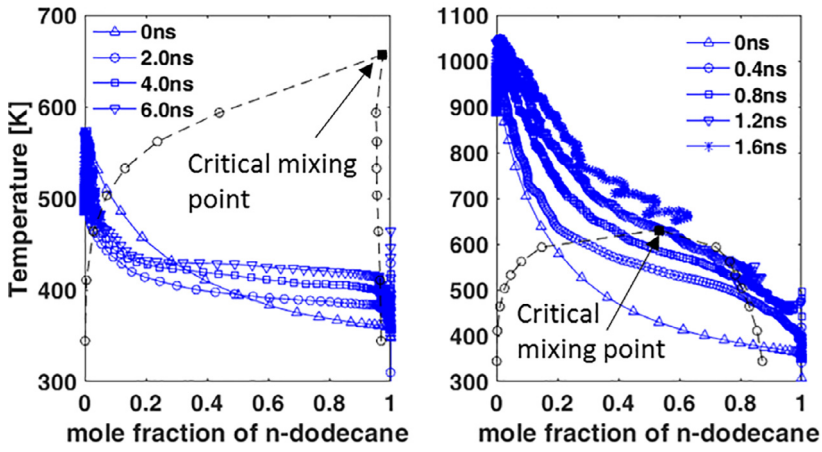

Fig. 5. Temperature as a function of mole fraction of n-dodecane and VLE diagram. (a) $T' = 0.91$, $p' = 1.21$, transition does not happen; (b) $T' = 1.67$, $p' = 5.96$, transition happens at $t = 1.2$ ns.

can be obtained. Figure 5 shows the correlation of these two properties at various time, together with the vapor-liquid equilibrium (VLE) line (dotted line) of the n-dodecane/nitrogen binary system under that pressure, which is obtained from the experimental results of García-Cordova et al. [32]. The $T - x_n$ line that increases beyond the critical mixing point (the peak of the VLE line) of the n-dodecane/nitrogen system indicates the time when the transition to supercritical state happens. As can be seen from Fig. 5, for low-temperature and low-pressure conditions ($T' = 0.91$, $p' = 1.21$ for example), supercritical transition cannot happen in the lifetime of the droplet. However, under high-temperature and high-pressure conditions like $T' = 1.67$, $p' = 5.96$, supercritical transition happened before evaporation ended.

By applying the above analysis to all the cases investigated, a regime diagram that indicates under what conditions the droplet can go supercritical can be determined. As shown in Fig. 6, the presented curve defines a boundary between the subcritical and supercritical evaporation regimes. Under the ambient conditions above this curve, transition to supercritical state happens at the droplet surface before evaporation ends. From Fig. 6 we can see that the minimum ambient pressure needed for supercritical transition decreases with increasing ambient temperature. This result is in agreement with many previous studies, including experimental measurements [35], continuum-based simulations [14,18] and molecular dynamics simulations [29].

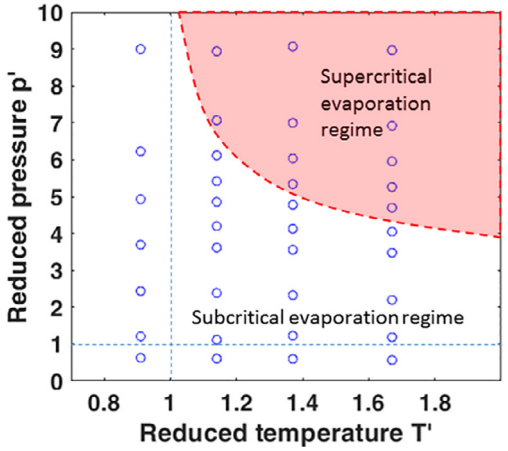

Fig. 6. Supercritical and subcritical evaporation regimes for medium-size droplet on the p-T diagram. The dots indicate the investigated cases with the ambient temperature and pressure combinations.

3.2. Effect of initial droplet size

Based on the conventional evaporation theory, d^2 decreases linearly with time during the quasi-steady state. Therefore, droplet lifetime should vary linearly with the square of the initial droplet diameter. In the present study, three droplets with various initial diameters (approx. 21 nm, 30 nm, 43 nm, respectively) were simulated under the same ambient conditions. For a direct comparison of the lifetime of various droplets, the evaporation lifetime is plotted as a function of the square of the initial droplet size (d_0^2) in Fig. 7. As indicated in Fig. 7, droplet lifetime increases almost linearly with d_0^2 for each ambient temperature and pressure combination.

In Fig. 8a the droplet d^2 histories of the three droplets under the same condition of $T' = 1.67$ and $p' = 5.96$ are plotted. Note here d^2 and time are both multiplied by a scale factor $d^2_{o,medium}/d_0^2$. Direct comparison of the d^2 curves indicates that evaporation rate constants for different droplets

Please cite this article as: G. Xiao, K.H. Luo and X. Ma et al., A molecular dynamics study of fuel droplet evaporation in sub- and supercritical conditions, Proceedings of the Combustion Institute, https://doi.org/10.1016/j.proci.2018.09.020

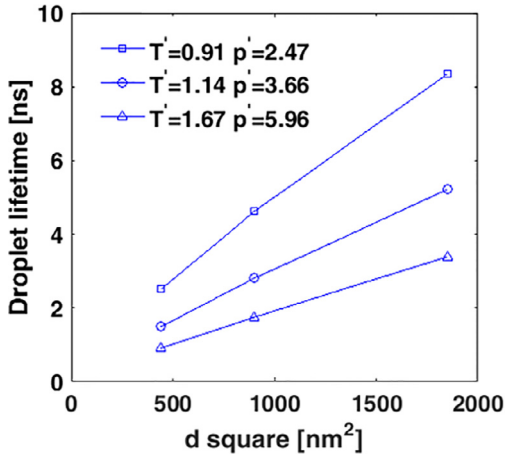

Fig. 7. Droplet lifetime as a function of droplet size.

are rather close. However, the heat-up time of the larger droplet makes up a smaller portion in the droplet lifetime. This is more positively indicated by Fig. 8b, in which the evaporation rate constants k of different droplets are almost identical under the same ambient condition, while normalized heat-up time τ_h (the ratio of actual heat-up time t_h and droplet lifetime t_L) decreases as droplet becomes larger. It is reasonable to expect that for large droplets in combustion devices, which are usually 2 to 3 orders of magnitude larger than the droplet investigated here, the heat-up time would be less prominent in the droplet lifetime. Figure 8c shows the heat-up time as a function of droplet size. A linear dependence of heat-up time with d_0 can be observed.

In Fig. 9, we plot the normalized transition time τ_T, which is the ratio between the supercritical transition time t_T and droplet lifetime t_L, as a function of reduced ambient pressure. All the cases where supercritical transition happens are shown. Note that the normalized transition time τ_T decreases with increasing ambient pressure and/or temperature. The dependence of τ_T on the ambient temperature can be attributed to faster heat transfer through the ambient to the droplet, when the ambient temperature is increased. The dependence of τ_T on the ambient pressure can be attributed to the increase in gas-phase thermal diffusivity in the near-critical regime [19], and the decrease in the critical mixing temperature when the ambient pressure is increased [18]. Moreover, it is evident that the normalized transition time of the larger droplet is shorter than that of the smaller droplet when the ambient pressure is relatively low ($p' < 5$). The effect of the initial droplet size on normalized supercritical transition time can be explained using the following equation,

$$\tau_T = \frac{t_T}{t_L} = \frac{t_T}{t_h + (t_L - t_h)} = \frac{b \cdot d_0}{a \cdot d_0 + c \cdot d_0^{\epsilon}} \tag{6}$$

Here, a, b, and c are constants. This is based on the present finding of a linear relationship between transition time t_T and heat-up time t_h, which increases linearly with d_0. On the other hand, $t_L - t_h$ is found to increase with droplet size at a rate higher than linear growth, that is, $t_L - t_h = c \cdot d_0^{\epsilon}$ with $\epsilon > 1$. As a result, we have $\tau_T = \frac{1}{\frac{a}{b} + \frac{c}{b} \cdot d_0^{\epsilon-1}}$. Therefore, with increasing droplet size d_0, normalized transition time decreases. This is more evident at lower pressure ($p' < 5$), while at higher pressure the difference between various droplets diminishes, as shown in Fig. 9. This finding is different from that of previous continuum-based simulations [18,19].

In addition, the minimum pressure needed for supercritical transition is higher for the smaller droplet than for the larger one. As shown in Fig. 10, the boundary between the subcritical and supercritical evaporation regimes extends to lower pressure conditions when the initial droplet diameter is increased. This phenomenon can be attributed to the decreasing normalized transition time with increasing droplet size at relatively low ambient pressure, which gives longer lifetime for the larger droplet to reach supercritical state (at $T' = 1.67$ & $p' = 3.57$, for example). The results in previous

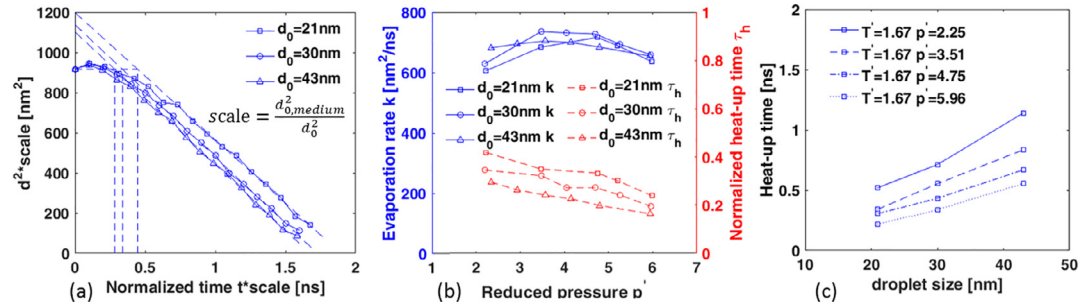

Fig. 8. (a) d^2 history of various sized droplet under $T' = 1.67$ and $p' = 5.96$, (b) evaporation rate constant and normalized heat-up time of various sized droplet under $T' = 1.67$, (c) droplet heat-up time as a function of initial droplet size.

Please cite this article as: G. Xiao, K.H. Luo and X. Ma et al., A molecular dynamics study of fuel droplet evaporation in sub- and supercritical conditions, Proceedings of the Combustion Institute, https://doi.org/10.1016/j.proci.2018.09.020

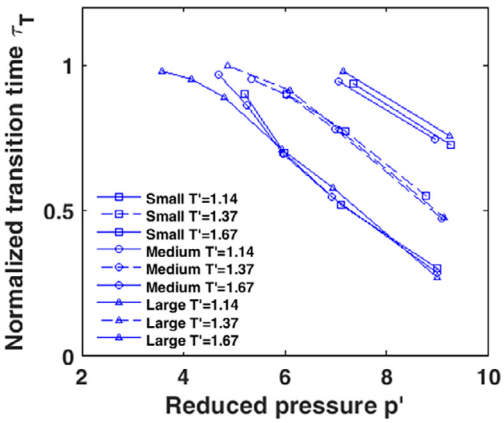

Fig. 9. Normalized transition time.

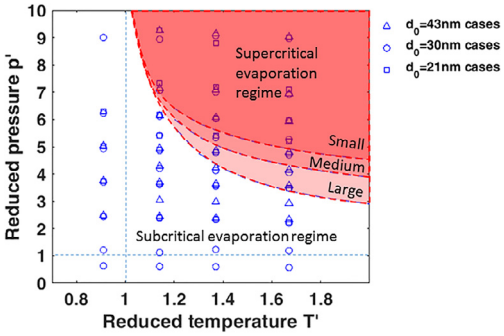

Fig. 10. Supercritical and subcritical evaporation regimes for droplets of different sizes. The dots indicate the investigated cases with the ambient temperature and pressure combinations.

continuum-based simulations [18,19] are consistent with the present finding, although the authors concluded that the boundary between the subcritical and supercritical evaporation regimes was independent of the droplet size. A possible explanation is that all macro-droplets (as investigated in [18,19]) have long enough a lifetime to reach supercritical state if the ambient temperature and pressure are high enough. Up to now, no experimental results are available to provide more insight into this issue.

To parameterize the dependence of minimum reduced pressure p' on the reduced temperature T' and droplet size d_0, we performed a classification of our dataset using the least squares solution for a regression model in the form $(p'-1) = a \cdot (T'-1)^b$. The investigated n-dodecane/nitrogen system exhibits supercritical evaporation regime over the space $(p'-1) > (-0.074d_0 + 5.09) \cdot (T'-1)^{-0.0138d_0+0.0042}$, as shown in Fig. 10.

4. Conclusions

Molecular dynamics simulations were used to investigate the evaporation process of an n-dodecane droplet in a nitrogen environment. Ambient conditions ranging from subcritical to supercritical with respect to the fuel and various initial droplet sizes were considered. Significant findings obtained in this study include:

1. Droplet lifetime decreases with increasing ambient pressure and/or temperature. Supercritical transition time decreases with increasing ambient pressure and/or temperature at a rate higher than that for droplet lifetime, since the normalized transition time decreases with increasing pressure and temperature.
2. The minimum ambient pressure needed for supercritical transition decreases with increasing ambient temperature. With increased droplet initial diameter, the boundary of supercritical regime extends to lower ambient pressures.
3. The droplet heat-up time as well as subcritical to supercritical transition time increases linearly with the initial droplet size d_0, while the droplet lifetime increases with d_0^2. Moreover, nano-droplets have unique features even though most of their characteristics are the same as macro-droplets. For example, the lifetime of nano-droplets can be too short for supercritical transition, even though the ambient temperature and/or pressure are in the supercritical regime.

Acknowledgments

Support from the Natural Science Foundation of China (Grant No. 91441120) is gratefully acknowledged. The simulations were performed on ARCHER funded under the EPSRC projects "UK Consortium on Mesoscale Engineering Sciences (UKCOMES)" (Grants No. EP/L00030X/1 and No. EP/R029598/1) and "High Performance Computing Support for United Kingdom Consortium on Turbulent Reacting Flow (UKCTRF)" (Grant No. EP/K024876/1).

References

[1] W. Mayer, A. Schik, B. Vielle, C. Chaveau, I. Gökalp, D. Talley, *J. Prop. Pow.* 14 (1998) 835–842.
[2] B. Chehroudi, D. Talley, E. Coy, *Phys. Fluids.* 14 (2002) 850–861.
[3] C.K. Law, *Prog. Energy Combust. Sci.* 8 (1982) 171–201.
[4] D.B. Spalding, *ARS J* 29 (1959) 828–835.
[5] V. Yang, N.N. Lin, J.S. Shuen, *Combust. Sci. Technol.* 97 (1994) 247–270.

Please cite this article as: G. Xiao, K.H. Luo and X. Ma et al., A molecular dynamics study of fuel droplet evaporation in sub- and supercritical conditions, Proceedings of the Combustion Institute, https://doi.org/10.1016/j.proci.2018.09.020

[6] K. Harstad, J. Bellan, *Int. J. Heat Mass Trans.* 41 (1998) 3537–3550.
[7] K. Harstad, J. Bellan, *Int. J. Multiph. Flow.* 26 (2000) 1675–1706.
[8] R. Matlosz, S. Leipziger, T. Torda, *Int. J. Heat Mass Transf.* 15 (1972) 831–852.
[9] D.E. Rosner, W.S. Chang, *Combust. Sci. Technol.* 7 (1973) 145–158.
[10] K.C. Hsieh, J.S. Shuen, V. Yang, *Combust. Sci. Technol.* 76 (1991) 111–132.
[11] E.W. Curtis, P.V. Farrell, *Combust. Flame.* 90 (1992) 85–102.
[12] H. Jia, G. Gogos, *J. Thermophys. Heat Trans.* 6 (1999) 738–745.
[13] J. Stengele, K. Prommersberger, M. Willmann, S. Wittig, *Int. J. Heat Mass Transf.* 42 (1999) 2683–2694.
[14] G.S. Zhu, S.K. Aggarwal, *Int. J. Heat Mass Trans.* 43 (2000) 1157–1171.
[15] G.S. Zhu, R.D. Reitz, S.K. Aggarwal, *Int. J. Heat Mass Trans.* 44 (2001) 3081–3093.
[16] G.S. Zhu, R.D. Reitz, *Int. J. Heat Mass Trans.* 45 (2002) 495–507.
[17] K. Harstad, J. Bellan, *Int. J. Multiph. Flow.* 26 (2000) 1675–1706.
[18] S.K. Aggarwal, C. Yan, G. Zhu, *Combust. Sci. Technol.* 174 (2002) 103–130.
[19] J.C. Oefelein, S.K. Aggarwal, *Proc. Cent. Turbul. Res.* (2000) 193–205.
[20] C.K. Law, F.A. Williams, *Combust. Flame.* 19 (1972) 393–405.
[21] C. Morin, C. Chauveau, P. Dagaut, I. Gökalp, M. Cathonnet, *Combust. Sci. Technol.* 176 (2004) 499–529.
[22] J. Sato, in: 31st Aerospace Science Meeting & Exhibit, AIAA, Reno NV, 1993 AIAA 93-0813.
[23] J.P. Hartfield, P.V. Farrell, *J. Heat Transfer.* 115 (1993) 699.
[24] H. Nomura, Y. Ujiie, H.J. Rath, J. Sato, M. Kono, *Symp. Combust.* 26 (1996) 1267–1273.
[25] H. Nomura, T. Murakoshi, Y. Suganuma, Y. Ujiie, N. Hashimoto, H. Nishida, *Proc. Combust. Inst.* 36 (2017) 2425–2432.
[26] T. Kadota, K. Satoh, D. Segawa, J. Sato, Y. Marutani, *Symp. Combust.* 27 (1998) 2595–2601.
[27] T.L. Kaltz, L.N. Long, M.M. Micci, et al., *Combust. Sci. Technol.* 136 (1998) 279–301.
[28] L. Consolini, S.K. Aggarwal, S. Murad, *Int. J. Heat Mass Trans.* 46 (2003) 3179–3188.
[29] G. Mo, L. Qiao, *Combust. Flame.* 176 (2017) 60–71.
[30] R.N. Dahms, J.C. Oefelein, *Proc. Combust. Inst.* 35 (2015) 1587–1594.
[31] B.Y. Cao, J.F. Xie, S.S. Sazhin, *J. Chem. Phys.* 134 (2011) 164309.
[32] T. García-Cordova, D.N. Justo-García, B.E. García-Flores, F. García-Sanchez, *J. Chem. Eng. Data.* 56 (2011) 1555–1564.
[33] S. Sanmartín, J. Ramos, J.F. Vega, J. Martínez-Salazar, *Eur. Polym. J.* 50 (2014) 190–199.
[34] G. Xiao, K.H. Luo, X. Ma, S. Shuai, *Commun. Comput. Phys.* 23 (4) (2017) 1241–1262.
[35] C. Crua, J. Manin, L.M. Pickett, *Fuel* 208 (2017) 535–548.

Please cite this article as: G. Xiao, K.H. Luo and X. Ma et al., A molecular dynamics study of fuel droplet evaporation in sub- and supercritical conditions, Proceedings of the Combustion Institute, https://doi.org/10.1016/j.proci.2018.09.020